Highly *n*-doped graphene generated through intercalated terbium atoms

L. Daukiya,[1,2] M. N. Nair,[3] S. Hajjar-Garreau,[1] F. Vonau,[1] D. Aubel,[1] J. L. Bubendorff,[1] M. Cranney,[1] E. Denys,[1] A. Florentin,[1] G. Reiter,[2] and L. Simon[1,*]

[1]*Institut de Sciences des Matériaux de Mulhouse, CNRS-UMR 7361, Université de Haute Alsace, 3Bis, rue Alfred Werner, 68093 Mulhouse, France*

[2]*Physikalisches Institut, Universität Freiburg, Hermann-Herder-Strasse 3, 79104 Freiburg, Germany*

[3]*Synchrotron SOLEIL-Ligne CASSIOPEE, L'Orme des Merisiers Saint Aubin, B.P. 48, 91192 Gif sur Yvette, France*

(Received 8 December 2017; revised manuscript received 11 January 2018; published 25 January 2018)

We obtained highly *n*-type doped graphene by intercalating terbium atoms between graphene and SiC(0001) through appropriate annealing in ultrahigh vacuum. After terbium intercalation angle-resolved-photoelectron spectroscopy (ARPES) showed a drastic change in the band structure around the *K* points of the Brillouin zone: the well-known conical dispersion band of a graphene monolayer was superposed by a second conical dispersion band of a graphene monolayer with an electron density reaching 10^{15} cm^{-2}. In addition, we demonstrate that atom intercalation proceeds either below the buffer layer or between the buffer layer and the monolayer graphene. The intercalation of terbium below a pure buffer layer led to the formation of a highly *n*-doped graphene monolayer decoupled from the SiC substrate, as evidenced by ARPES and x-ray photoelectron spectroscopy measurements. The band structure of this highly *n*-doped monolayer graphene showed a kink (a deviation from the linear dispersion of the Dirac cone), which has been associated with an electron-phonon coupling constant one order of magnitude larger than those usually obtained for graphene with intercalated alkali metals.

DOI: 10.1103/PhysRevB.97.035309

I. INTRODUCTION

Based on the possibility of intercalation of various atoms, strongly inspired by the results observed in graphite intercalation compounds and motivated by possible superconductivity observed for such intercalated systems, graphene became the investigation playground for a large variety of alkali metals such as Li, K, Ca, Cs, and Rb [1–5]. For graphene, particularly for epitaxial graphene on silicon carbide (SiC), the band dispersion after intercalation can be measured by angle-resolved-photoelectron spectroscopy (ARPES). For most of the above-mentioned elements a complex band structure was found, showing a combination of a new linear highly *n*-doped dispersion and the dispersion of pristine monolayer graphene. The new dispersion curve was attributed either to a decoupling of the buffer layer or to the doping of monolayer graphene on top when no intercalation was expected [6]. However, no systematic studies were performed to prove these assumptions experimentally or to try to distinguish the contribution of each graphene layer and to isolate the highly *n*-doped graphene. Indeed, it is not really clear how the type of element modifies the Fermi level of highly *n*-doped graphene, whether the observed two bands correspond to the mixing of the band structures of two separated graphene layers, or whether it could be associated with a new type of stacking of graphene layers as proposed by Kim *et al.* [6]. In the case of the intercalation of alkali metals a kink (a deviation of the linear dispersion band near the Fermi level) was observed and discussed in terms of electron-phonon coupling in the framework of the BCS theory of superconductivity. For these elements, the strength of electron-phonon coupling was systematically studied and found to depend on the density of transferred electrons [7]. In our study we focus on much more rarely studied lanthanide elements. Previous studies have measured the band structure of graphene with intercalated ytterbium [8] and, more recently, Ce [9]. In both cases a complex band structure is observed and in the case of ytterbium a faint highly *n*-doped Dirac cone was also observed but a possible electron-phonon coupling was neither observed nor discussed.

In this work we examine intercalation of terbium atoms (Tb) atoms using epitaxial graphene on SiC(0001). Using x-ray photoelectron spectroscopy (XPS) and ARPES, we show the appearance of a highly *n*-doped graphene after intercalation of Tb atoms. Monolayer (ML) graphene on SiC(0001) consists of two graphene layers. One is partially covalently bonded to the upper silicon atoms of the SiC substrate. This is called the buffer layer (BL), which is covered with a true ML of graphene on top. After intercalation, ARPES spectra exhibited a complex band structure with a contribution from a highly *n*-doped graphene layer. XPS measurements revealed that the intercalated Tb remained metallic and suggested that it was protected against oxidation. We also observed no Tb-C bond formation. Intercalation occurred also below the BL, generating the highly *n*-doped graphene layer. In contrast to previous studies, we were able to clearly distinguish the origin of the two dispersion bands and showed that it is possible to form a single highly *n*-doped ML graphene. The observed strength of the electron-phonon coupling was one order of magnitude higher than expected for intercalated alkali metal with our doping level [7].

*Laurent.simon@uha.fr

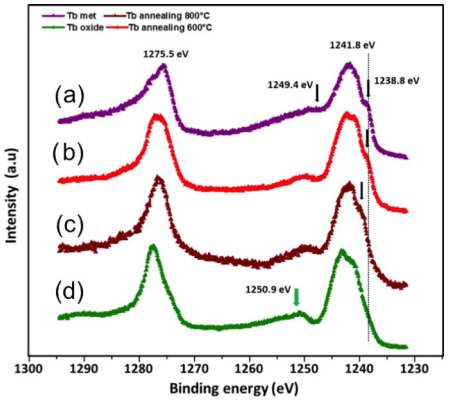

FIG. 1. XPS spectra of the Tb3d core level. (a) Just after deposition. After annealing (b) at 600°C and (c) at 800°C. (d) Oxidized Tb.

II. EXPERIMENTAL METHODS

Monolayer graphene samples were prepared by annealing of 6H-SiC(0001) at 1100°C and a base pressure of 1×10^{-10} mb. By varying the annealing time and temperature, we were able to prepare samples with different ratios of graphene to buffer layer. The Tb atoms were deposited by electron-beam evaporation in ultrahigh vacuum (UHV) at a base pressure of 8×10^{-10} mb. The deposition rate was monitored by quartz-crystal microbalance. We deposited a terbium layer of approximately 0.3 nm. After deposition of terbium, samples were annealed at 600°C for 10 mins. Subsequent annealing for 1 h resulted in intercalation of terbium atoms. In-house physical characterizations were performed in UHV by low-energy electron diffraction (LEED), by scanning tunneling microscopy (STM), and by photoelectron spectroscopy techniques (XPS, ARPES). LEED experiments were performed *in situ* with an Omicron SpectaLEED. STM experiments were performed *in situ* with an LT-STM from Omicron at 77 K and a base pressure in the 10^{-11} mb range. Images were acquired in the constant-current mode with bias voltage applied to the sample and employing chemically etched W tips. Photoelectron spectroscopy (XPS, ARPES) measurements were performed *in situ* using a VG Scienta R3000 spectrometer equipped with a hemispherical analyzer. An energy resolution of 16 meV is reached with a pass energy of 20 eV. For XPS we used a monochromatic x-ray source (AlKα, 1486.6 eV), and for ARPES a UV source HeII (40.8 eV). For more clarity, periodicity expressed with respect to SiC(0001) and graphene is referred to in the following as -SiC and -G, respectively.

III. RESULTS AND DISCUSSION

Once deposited, terbium atoms, which are highly reactive, get progressively oxidized, even in UHV as shown by the Tb3d core level peaks in Fig. 1. Just after deposition the Tb3d core level spectra displayed a metallic character, as shown in Fig. 1(a). Two components of the spectra, located around 1241.8 and 1275.5 eV, were attributed to Tb3d5/2 and Tb3d3/2 with a spin-orbit coupling of 33.7 eV, respectively. The metallic character was evidenced by multiplet splitting in the photoemission process due to the unfilled shell at the 4f core level [10]. These multiplets were well defined at 1238.8 and 1249.4 eV as indicated by arrows in Fig. 1. The O1s component in the XPS spectra increased over time, multiplet splitting disappeared, and an oxidized Tb3d peak emerged at 1250.9 eV as shown in Fig. 1(d). This is attributed to the effect of hydridization between the final state 4f and the O2p core level [11]. After annealing at 600°C, the amount of oxide was reduced and the Tb3d core level peak again showed a more pronounced metallic character [Fig. 1(b)]. However, this Tb layer was not stable in time and oxidized again even in UHV. After annealing at 800°C [Fig. 1(c)], contributions from oxides were completely removed. The resulting structure was stable in UHV. This suggests that the Tb atoms were intercalated below the graphene layer and so were protected against oxidation. Figure 2 displays the C1s core level peak of pristine graphene [Fig. 2(a)] and after intercalation of Tb atoms [Fig. 2(b)]. A scheme for ML graphene with a BL on SiC(0001) is shown in Fig. 2(c). The typical C1s core level peak shows four components [Fig. 2(a)]. One, labeled SiC, corresponds to carbon atoms in the SiC substrate at 283.76 eV and the C-sp2-G component at 284.68 eV corresponds to the top graphene monolayer. The BL is a graphene layer partially covalently bonded to the underlying SiC substrate and contributes to two components: S1-sp3 at 285.02 eV is attributed to covalently bonded carbon atoms, and S2-sp2 at 285.62 eV to C-C bonds in the BL. After intercalation as shown in Fig. 2(b), the C-sp2-G component did not change. However, the contribution of the SiC component was shifted by 0.36 eV towards lower energies, attributed to the modification of the work function due to the presence of the intercalated terbium

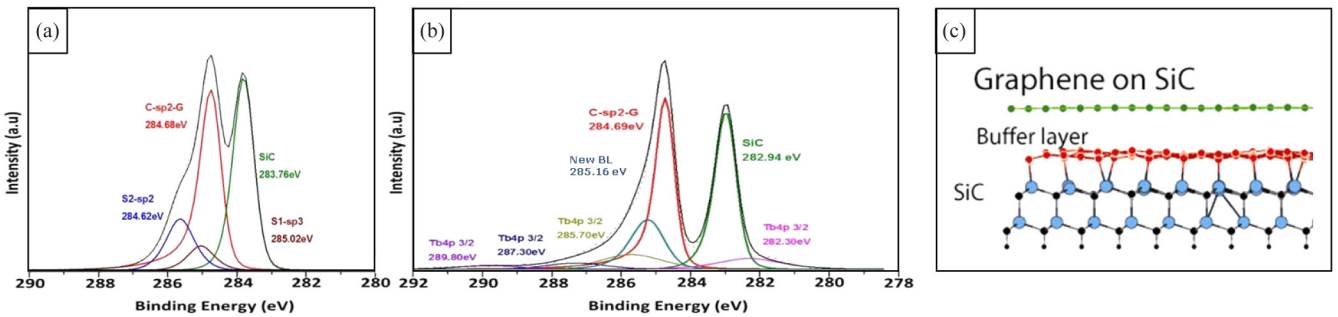

FIG. 2. XPS spectra of the C1s core level (a) of pristine monolayer graphene and (b) after terbium intercalation. (c) Scheme of ML graphene on SiC(0001).

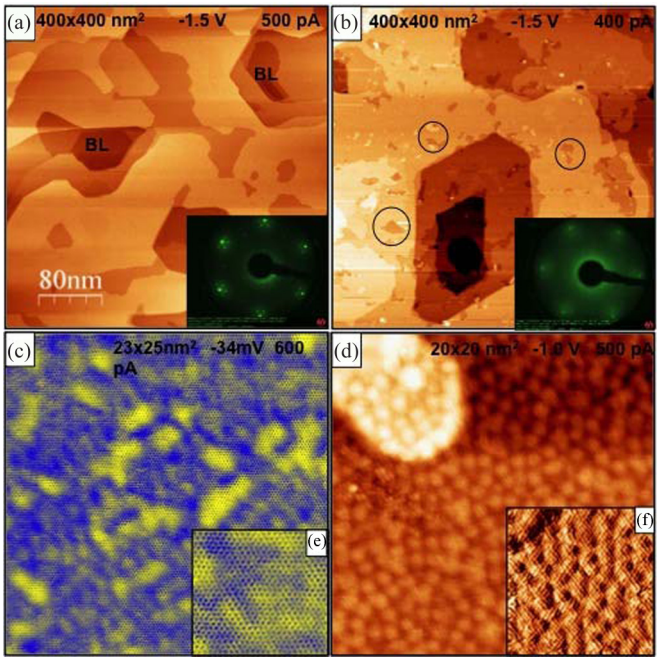

FIG. 3. STM images and corresponding LEED pattern of (a) pristine graphene on SiC (0001) before intercalation experiments and (b) graphene intercalated with terbium atoms and annealed at 800°C. (c) STM image of a terrace after terbium intercalation, where the further zoom-in shows all six carbons of graphene in (e). (d) STM image of a recessed area after terbium intercalation, where the further zoom-in shows all six carbons of graphene in (f).

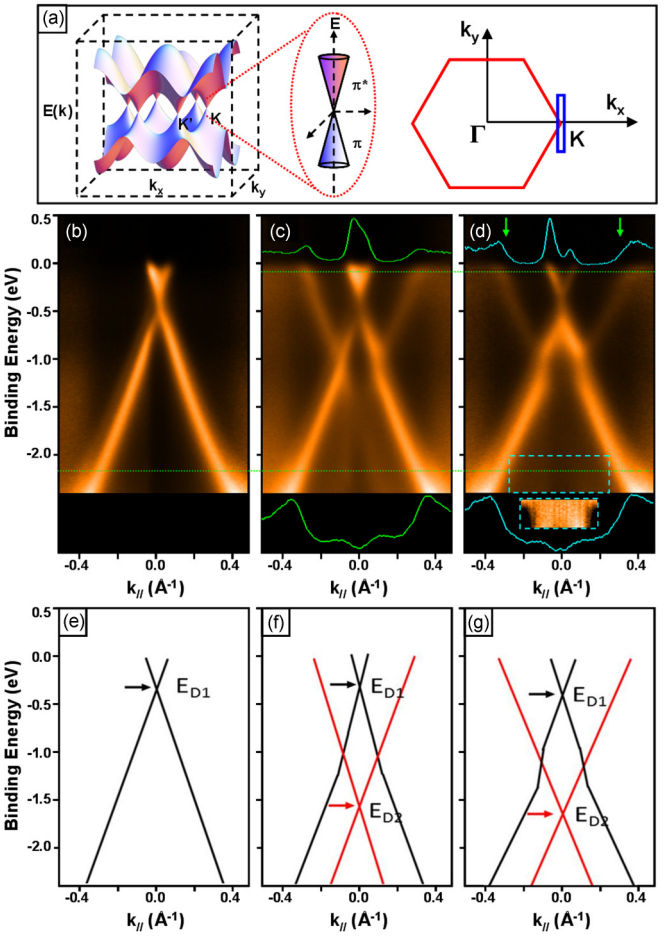

FIG. 4. (a) Schemes of the graphene reciprocal lattice and the K point where the ARPES spectra are acquired. ARPES spectra (b) of pristine graphene and after deposition of Tb and annealing at 800°C (c) for 5 min and (d) for 30 min. In (c) and (d), line scans along different energies (near E_f and near -2.4 eV) are represented, in order to show clearly the existence of a new band structure, in particular, in the lowest part of the ARPES spectra. Inset in (d): A short window represented by the dashed-line rectangle in order to increase the contrast locally. (e–g) Corresponding schemes showing an increase in the Fermi surface of the new band with the annealing time, as evidenced by the line scan near E_f in (d), where green arrows represent the positions of the new band in the line scan near E_f in (c).

atoms on top of the SiC substrate. Such observations were also made for the intercalation of other elements [8,12]. The contribution of Tb4p3/2 is at the same position as that of C1s. Following the procedure proposed by Padalia *et al.* [10], we deconvoluted all components in the spectra resulting from strong multiplet splitting and C1s, respecting the atomic ratio. After Tb intercalation it was not possible to identify the components S1-sp3 and S2-sp2 of the BL. However, a new component, labeled "new BL," emerged at 285.16 eV suggesting the formation of a new layer resulting from the decoupling of the BL from SiC after the intercalation of Tb atoms.

Figure 3 displays the STM and LEED measurements done on pristine epitaxial ML graphene [Fig. 3(a)] and after intercalation of terbium atoms [after deposition and annealing at 800°C; Figs. 3(b) to 3(f)]. The pristine graphene consists of large areas of ML graphene as schematized in Fig. 2(c), with some portion of buffer layer graphene (typically less than a few percent), which appears darker in the figure (labeled BL). The LEED pattern in the inset shows the typical 1×1-G diagram surrounded by the so-called 6×6-SiC reconstruction, which is due to the BL reconstruction under the ML graphene. After intercalation of terbium, terraces are no more well defined but seem to be indented-like, with small recessed areas observed everywhere (less than 10% of the surface; circled in Fig. 3(b)], at the former positions of BL areas and even in the middle of terraces. Figures 3(c) and 3(d) are zoom-ins on the top of a terrace and on the recessed area, respectively. The corresponding insets [Figs. 3(e) and 3(f)], showing all six C atoms, confirm the presence of a graphene layer on top of the intercalated structures, a layer which is more corrugated in the case of Fig. 3(d). In both cases the BL 6×6-SiC reconstruction has disappeared and intercalated terbium atoms (below the ML and BL) are not ordered. The absence of underlying reconstruction confirms that the BL is completely decoupled from the substrate. This is proven as well by the LEED pattern in Fig. 3(b), which shows the 1×1-G pattern, with the 6×6-SiC spots no longer visible.

ARPES spectra for pristine ML graphene [shown in Fig. 4(b)], taken along the ΓK direction as shown in the schematic in Fig. 4(a), showed typical dispersion of the π band, with the Dirac point 0.45 eV below the Fermi level due to n doping from the substrate [13] (n doping $= 1 \times 10^{13}$ cm^{-2}). After

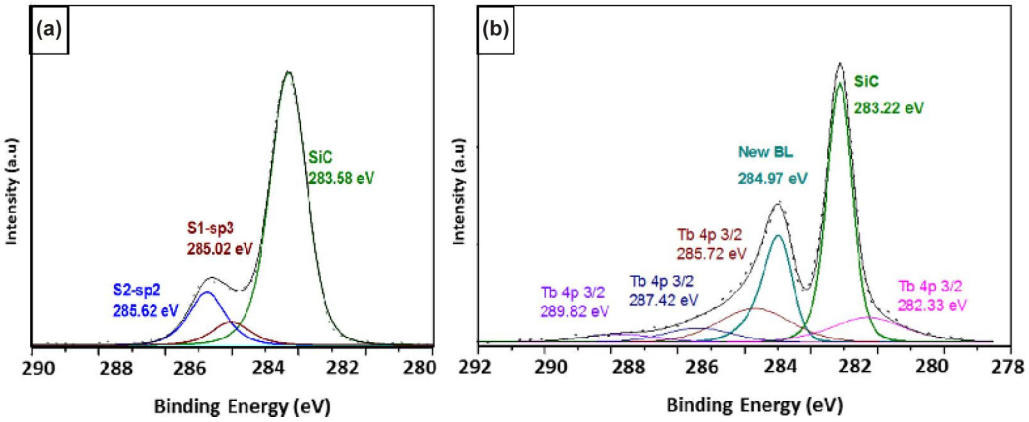

FIG. 5. C1s core level spectra (a) of pristine buffer layer and (b) after Tb intercalation.

deposition of terbium atoms, no dispersion was observed by ARPES around the K points, which demonstrates that terbium atoms completely covered the graphene layer. After annealing at 800°C a modification of the band structure was observed. The ARPES spectra showed that the contribution from pristine graphene to the dispersion curve was then accompanied by a new band with a large Fermi surface, as shown in Fig. 4(b). The n doping and the Fermi surface of this new band increased when the sample was additionally annealed at 800°C for 1 h [see Fig. 4(c)]. The resulting complex band structure can be interpreted as the superposition of two dispersion curves originating from two distinct graphene layers, as previously discussed for intercalation of ytterbium and aluminum [8,12] or for the upper graphene layer on top of bilayer graphene after doping [6]. The schemes in Figs. 4(e) to 4(g) provide a simplistic interpretation of the ARPES spectra, where the dispersion curve resulting from the initial graphene layer is shown in black. The Dirac point (E_{D1}) of the initial graphene layer remained located 0.45 eV below the Fermi level. The dispersion curve corresponding to the new graphene layer is represented by the red line. This new graphene layer had a large Fermi surface, increasing with the annealing time, and a Dirac point (E_{D2}) located 1.57 eV below the Fermi level, as shown in Figs. 4(f) and 4(g).

The Fermi velocity (v_F) of pristine graphene was measured to be around $0.83 \pm 0.07 \times 10^6$ m s^{-1}. v_F and E_{D2} of the new graphene layer observed after 10 min of annealing at 800°C were $0.80 \pm 0.09 \times 10^6$ m s^{-1} and -1.57 eV, respectively. After annealing at 800°C for 1 h, v_F and E_{D2} changed to $0.65 \pm 0.07 \times 10^6$ m s^{-1} and -1.59 eV, respectively. The density of electrons at the Fermi level can be calculated by the following relation between E_D and v_F as

$$n_e = \frac{E_D^2}{\pi \hbar^2 v_F^2}. \quad (1)$$

Using Eq. (1) the electron density calculated for the pristine graphene is 2.6×10^{13} cm^{-2}. The electron density for the new graphene is around 4.3×10^{14} cm^{-2}.

An important question in this study concerns the origin of this new graphene layer. In earlier intercalation studies on graphene, highly n-doped spectra were always attributed to the decoupling of the buffer layer from the underlying SiC substrate. However, to the best of our knowledge, no clear experimental evidence was provided. The contributions of pristine ML graphene and highly n-doped graphene to the band structure have never been separated. In order to identify the exact nature of the component labeled "new BL" we have generated a pure pristine buffer layer for which we studied the decoupling of the buffer layer resulting from the intercalation of terbium atoms. Samples of pristine buffer layer were prepared by annealing of SiC substrates at 900°–1000°C in UHV at a base pressure of 1×10^{-10} mb. The corresponding C1s core level spectrum is shown in Fig. 5(a). We observed only three components, the SiC peak and components S1-sp3 and S2-sp2, corresponding to the BL. After terbium intercalation, XPS spectra revealed a clear modification of the buffer layer, confirming the deconvolution done previously on the C1s core level peaks for the ML graphene after intercalation of terbium atoms. Figure 5(b) shows the C1s core level spectrum after intercalation of terbium atoms under buffer layer graphene. The peaks S1-sp3 and S2-sp2 corresponding to the BL have again disappeared and the peak called new BL is clearly observable at 285 eV. A slight shift, around 0.36 eV, toward a lower energy was observed for the C1s peak of SiC. The full width at half-maximum (FWHM) of this peak was 0.97 eV, which is larger than that of the C-Sp2-G peak of the graphene layer (0.65 eV). We attribute this increase in FWHM to inhomogeneities of the doping across the whole sample.

In order to clearly confirm that the new structure of the buffer layer corresponds to a highly n-doped graphene layer as observed in the previous complex band structure found by ARPES, we have systematically varied the graphene–to–buffer layer ratio in the pristine samples before terbium intercalation by adjusting the annealing conditions. We have prepared samples with ratios of graphene to buffer layer of 80/20, 50/50, 30/70, and 0/100 and performed intercalation of terbium atoms under the same conditions for every sample. The graphene–to–buffer layer ratio can be verified by the C1s core level spectra, acquired from the samples before intercalation experiments, shown in Figs. 6(a) to 6(d). The resulting ARPES curves are shown in Figs. 6(e) to 6(h).

The intensity of the new n-doped graphene dispersion band increased with increasing percentage BL content of the sample, while the contribution of the pristine graphene layer

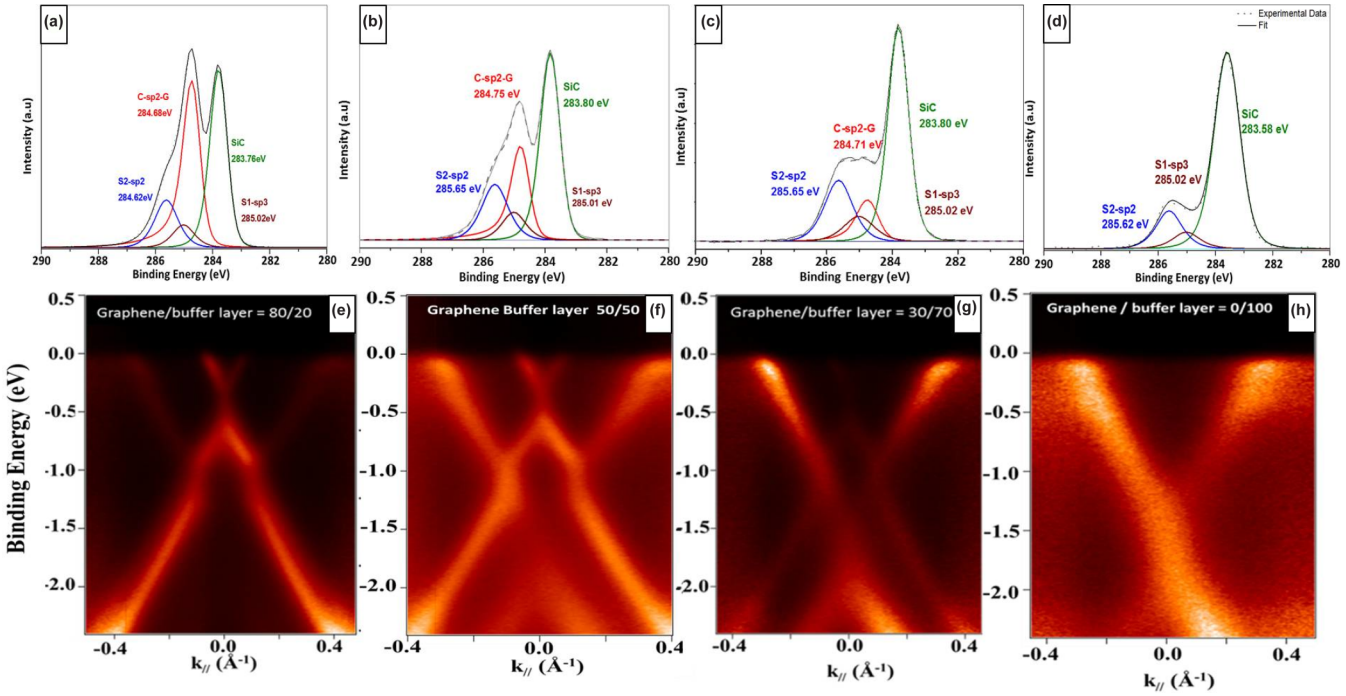

FIG. 6. C1s core level spectra of pristine graphene samples with varying graphene–to–buffer layer (BL) ratios: (a) 80/20; (b) 50/50; (c) 30/70; (d) 0/100. (e–h) Resulting ARPES spectra after terbium intercalation on these samples. This clearly shows that the new highly n-doped band structure results from the decoupling of BL by intercalated terbium atoms.

disappeared. Finally, for the sample with 100% buffer layer a single dispersion curve was observed, which corresponds to a highly n-doped graphene layer. This confirms that the origin of this highly n-doped band has to be attributed to the decoupling of the buffer layer caused by intercalation of Tb atoms. We show also that it is possible to synthesize an isolated highly n-doped graphene layer with a level of doping which can reach 10^{15} cm^{-2}, a value similar to values obtained by ionic liquid doping.

Then a second question arises, about the origin of the second band shown in Figs. 4(c) and 4(d) and schematized by the black curves in Figs. 4(f) and 4(g). Indeed, we may assume that it is due to the presence of areas of pristine monolayer graphene remaining after the intercalation of terbium atoms, as its ARPES spectrum looks like that of pristine monolayer graphene shown in Fig. 4(b). But XPS and LEED results have proven that BL is decoupled everywhere by Tb atoms. In this case, the band structure in ARPES should be more parabolic (more massive fermions) and STM images at a low bias should resolve every second C atom of the top ML, as in the case of bilayer graphene in A-B stacking. ARPES spectra shown in Figs. 4(c) and 4(d) having linear dispersion and STM images, where all six C atoms are imaged [see Figs. 3(b), 3(c), and 3(e), representing more than 90% of the surface], rule out this possibility. Moreover, disordered intercalated structures are clearly visible under the ML. Our observations strongly support the conclusions of K. S. Kim *et al.* [6] and recent calculations done in the case of Yb intercalation by M. Kim *et al.* [14], where it is supposed that the intercalation between the bottom and the top graphene layer perturbs the stacking, leading to A-A stacking. We must here conclude that intercalation happens everywhere on the sample surface, under the buffer layer, and also between the top and the bottom graphene layer.

In addition, a kink near the Fermi level was observed in the ARPES results. As shown in Fig. 3(c), it became more pronounced when both band structures were observed. Such a kink may reveal collective excitations and possible electron-phonon coupling. The electron-phonon coupling strength (λ) is a key parameter in the determination of the critical temperature of superconductivity in the framework of the BCS theory, particularly for graphite/graphene intercalation compounds [15]. The strength of electron-phonon coupling depends on the density of states at the Fermi level, on the phonon frequency mode, and on how much the intercalated atoms are able to bend the in-plane graphene vibrations into out-of-plane graphene phonon mode (deformation potentials). In a systematic study of λ as a function of the intercalated alkali metals for graphene compounds, Fedorov *et al.* [7] found experimental evidence of a dependence of λ on the density of electron D at the Fermi level following the relation $\lambda = 10^{-9}\sqrt{D}$, with D in cm^{-2}. They found for the highest electron density in their system, 5×10^{14} cm^{-2}, a value of $\lambda = 0.16$. Considering the highly n-doped graphene layer, and under the hypothesis that the kink would be associated with electron-phonon coupling and not another electron-electron correlation effect, we have extracted the electron-phonon coupling strength from ARPES measurements following the method used by Fedorov *et al.* [7] and found $\lambda = 1.2$. This value is one order of magnitude higher than the one expected in the case of alkali metals. Indeed for our level of electron doping, reaching 10^{15} cm^{-2}, we should expect $\lambda = 0.25$ [7]. As discussed in [7] such a high value of λ indicates either a possible ordering of the intercalated species, the involvement of more than one layer of graphene (this is

the case for graphite intercalation compounds), or a reduced distance between the intercalated atoms and the graphene layer.

IV. CONCLUSIONS

In conclusion, we have performed the intercalation of terbium atoms under the epitaxial graphene on SiC(0001). Using ARPES, XPS, and STM measurements, we have shown that terbium atoms can be intercalated under the buffer graphene layer, which is transformed in a new graphene monolayer with a doping level reaching 10^{15} cm^{-2}. This doping level is of the order of magnitude of the highest doping level achieved with an ionic liquid gate field. A strong electron-phonon coupling strength λ is deduced from APRES measurements. Compared to other systems, particularly to the intercalated alkali metals which have been systematically studied and for which superconductivity has been observed, our value is one order of magnitude higher than expected for our high doping level and also higher than that for graphite intercalation compounds. Of course the link with superconductivity is not determined here but these values exemplarily demonstrate the appeal of terbium as an intercalated element. Further work is required to improve the homogeneity of the sample and then perform transport measurements. The role of terbium coverage, the intercalation temperature, and how n doping occurs have to be studied systematically.

ACKNOWLEDGMENTS

This work was supported by the Région Alsace, the CNRS and the Université Franco-Allemande. The Agence Nationale de la Recherche supported this work under the ANR Blanc program, reference ANR-2010-BLAN-1017-ChimiGraphN.

[1] K. Sugawara, K. Kanetani, T. Sato, and T. Takahashi, AIP Adv. **1**, 022103 (2011).
[2] C. Virojanadara, S. Watcharinyanon, A. A. Zakharov, and L. I. Johansson, Phys. Rev. B **82**, 205402 (2010).
[3] S. Ichinokura, K. Sugawara, A. Takayama, T. Takahashi, and S. Hasegawa, ACS Nano **10**, 2761 (2016).
[4] S. Watcharinyanon, C. Virojanadara, and L. I. Johansson, Surface Sci. **605**, 1918 (2011).
[5] M. Petrovic, I. Srut Rakic, S. Runte, C. Busse, J. T. Sadowski, P. Lazic, I. Pletikosic, Z.-H. Pan, M. Milun, P. Pervan, N. Atodiresei, R. Brako, D. Sokcevic, T. Valla, T. Michely, and M. Kralj, Nat. Commun. **4**, 2772 (2013).
[6] K. S. Kim, A. L. Walter, L. Moreschini, T. Seyller, K. Horn, E. Rotenberg, and A. Bostwick, Nat. Mater. **12**, 887 (2013).
[7] A. V. Fedorov, N. I. Verbitskiy, D. Haberer, C. Struzzi, L. Petaccia, D. Usachov, O. Y. Vilkov, D. V. Vyalikh, J. Fink, M. Knupfer, B. Büchner, and A. Grüneis, Nat. Commun. **5**, 3257 (2014).
[8] S. Watcharinyanon, L. I. Johansson, C. Xia, J. I. Flege, A. Meyer, J. Falta, and C. Virojanadara, Graphene **2**, 66 (2013).
[9] J. Kim, P. Lee, M. Ryu, H. Park, and J. Chung, RSC Adv. **6**, 114219 (2016).
[10] B. D. Padalia, W. C. Lang, P. R. Norbis, L. M. Watson, and D. J. Fabian, Proc. R. Soc. Lordon A **354**, 269 (1977).
[11] A. Kotani and H. Ogasawara, J. Electron Spectrosc. Relat. Phenom. **60**, 257 (1992).
[12] C. Xia, L. I. Johansson, A. A. Zakharov *et al.*, Mater. Rese. Express **1**, 015606 (2014).
[13] M. N. Nair, M. Cranney, F. Vonau, D. Aubel, P. Le Fèvre, A. Tejeda, F. Bertran, A. Taleb-Ibrahimi, and L. Simon, Phys. Rev. B **85**, 245421 (2012).
[14] M. Kim, M. C. Tringides, M. T. Hershberger, S. Chen, M. Hupalo, P. A. Thiel, C.-Z. Wang, and K. M. Ho, Carbon **123**, 93 (2017).
[15] G. Profera and F. Mauri, Nat. Phys. **8**, 131 (2012).